Soil & Tillage Research 244 (2024) 106214

Contents lists available at ScienceDirect

Soil & Tillage Research

journal homepage: www.elsevier.com/locate/still

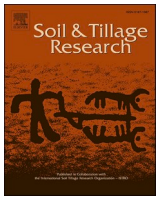

# Traction modifies the contact area and the vertical and horizontal stress distributions beneath the tyre

Loraine ten Damme [a,b,*], Alvaro Calleja-Huerta [a], Lars Juhl Munkholm [a], Per Schjønning [a], Thomas Keller [b,c], Mathieu Lamandé [a]

[a] Aarhus University, Department of Agroecology, Research Centre Viborg, Blichers Allé 20, P.O. Box 50, Tjele DK-8830, Denmark
[b] Swedish University of Agricultural Sciences (SLU), Department of Soil and Environment, Box 7014, Uppsala SE-75007, Sweden
[c] Agroscope, Department of Agroecology and Environment, Reckenholzstrasse 191, Zürich CH-8046, Switzerland

ARTICLE INFO

*Keywords:*
Contact stress
Drawbar pull
Soil compaction risk assessment
Stress-state
Tyre-soil interaction

ABSTRACT

Improving the prediction accuracy of the risk of soil structure deformation during wheeling requires a better understanding of the effects of traction on the vertical and horizontal stress distributions beneath tyres. In this study, these distributions were assessed for a rear wheel of a pulled (i.e., passive) and pulling (i.e., active) tractor during wheeling. The total load of the tractor was 85.2 kN, with a static rear wheel load of 33.0 kN on a 650/60 R38-tyre, inflated to 80 kPa. The 4WD was disabled in the active configuration. Vertical and horizontal contact stresses were measured at a frequency of 1 kHz using pressure transducers at 0.10 m depth of a sandy loam agricultural soil, covering a width of about 0.75 m, thereby capturing the entire stress distribution beneath the tyre. With these data, the contact characteristics (apparent wheel load, contact area, mean ground pressure) were calculated, the stress distributions characterised, and the ratio of horizontal to vertical stress for numerous positions beneath the rear tyre obtained. The results show that traction modifies the tyre-soil interaction significantly. The tyre-soil contact area was larger and the magnitude of vertical stress was lower for the active than for the passive tyre. On the other hand, the magnitude of horizontal stress was higher for the active than for the passive tyre. Consequently, the ratio of horizontal over vertical stress was higher beneath the active than beneath the passive tyre ($P < 0.001$), with median values of 1.0 and 0.5, respectively. Vertical and horizontal stress peak values did not spatially align but occurred in different positions beneath the active tyre. These findings thus contradict the assumption that horizontal stress near the tyre-soil interface is simply a function of vertical stress. Traction changed the distribution of vertical stress at the tyre-soil interface, with vertical stress peaking in different positions beneath the tyres, whilst the effects of traction on the horizontal stress was primarily related to the magnitude. The results of this study highlight the importance of incorporating different drive modes in predictions of the stress-state beneath a tyre and thus the assessment of the risk of soil deformation induced by wheeling.

## 1. Introduction

Agricultural soils are often exposed to high mechanical stresses from wheeling in field operations (Arvidsson et al., 2003; Keller et al., 2019), which carries a considerable risk of soil structure degradation. This, in turn, has adverse consequences for many soil processes and functions as well as for crop growth (Håkansson and Reeder, 1994; Horn and Peth, 2011). When the magnitude of stress exceeds a soil's internal strength, volumetric straining, shearing, or (usually) a combination of these two processes occur (Horn et al., 1998). The soil deformation process that potentially prevails during wheeling depends on the soil stress-state induced by the passing wheel, on the stress propagation through the soil, and on soil strength. A proper assessment of the overall risk of soil structure degradation thus requires a thorough understanding of the stress-state during wheeling.

Several assessment tools are available to limit the risk of soil compaction, such as the Soil Compaction Model "SOCOMO" (Van den Akker, 2004; Van den Akker and Van Wijk, 1987), SoilFlex (Keller et al., 2007) and the Terramechanical model "Terranimo ®" (Stettler et al., 2014). These common assessments usually first estimate the vertical

* Corresponding author at: Aarhus University, Department of Agroecology, Research Centre Viborg, Blichers Allé 20, P.O. Box 50, Tjele DK-8830, Denmark.
*E-mail address:* ltd@agro.au.dk (L. ten Damme).

https://doi.org/10.1016/j.still.2024.106214
Received 21 March 2024; Received in revised form 11 June 2024; Accepted 13 June 2024
Available online 19 June 2024

contact stress distribution from static loading characteristics (e.g., wheel load, tyre dimensions, inflation pressure), then simulate stress propagation following concepts outlined by Boussinesq (1885) and Söhne (1953), and finally assess the risk of soil compaction by comparing the local magnitude of vertical stress with soil compressive strength (i.e., precompression stress).

SOCOMO and SoilFlex also evaluate the risk of soil shearing using the Mohr Coulomb failure criterion, i.e., based on the major and minor principal stresses and the soil's angle of internal friction and cohesion (Keller et al., 2007; Van den Akker, 2004). These tools can be used to calculate the horizontal pressure distribution on the soil surface and the full stress state at any position in the soil, whereby the horizontal stress distribution at the soil-tyre interface can be estimated following various principles (e.g., following the vertical stress distribution, linearly or uniform). However, the distribution of horizontal stress at the soil-tyre interface and the risk of soil shearing are not properly validated against measured data.

Soil compaction risk assessments are typically based on rolling or driving, but not pulling wheels. Thus, assessments neglect the knowledge that the drive mode (rolling, braking or pulling) of a wheel affects the stress state beneath the tyre (Pytka, 2009; Soane et al., 1981; Yong and Foda, 1990). Pulling requires a tractive force and wheel slip. This induces additional shear stresses in the soil beneath a tyre and increases the risk of shear deformation (Pytka, 2009; Way et al., 2005). Following Horn et al. (1989), the amount of shear stress applied to soil can be estimated from the magnitudes of vertical and horizontal stress: ratios of horizontal to vertical stress both smaller and bigger than 1 reflect shear stress. The availability of experimental data on the stress-state beneath pulling wheels is, however, limited. While authors such as Bailey et al. (1996), Peth and Horn (2006), Pytka (2005), Seehusen et al. (2014), Way et al. (2005) and Wiermann et al. (1999) used a stress state transducer with six pressure cells that allowed calculations of the complete stress state during wheeling, data specifically on the horizontal stress distribution beneath tyres are scarce (Acquah and Chen, 2023; Calleja-Huerta et al., 2023; De Pue et al., 2020a, 2020b; Ten Damme et al., 2021b).

Tyres without a pulling force typically have an axes-symmetrical contact area that can be described by a super-ellipse, with a half-length and a half-width (Hallonborg, 1996; Lamandé and Schjønning, 2008; Schjønning et al., 2008). An axes-symmetric shape allows analyses of the effects of different loading characteristics on the size of the tyre-soil contact area without considering potential differences in the length of the contact area in front of and behind the axle. Perhaps this is the reason why many studies have focussed on the effects of, for example, loading conditions on the size of the tyre-soil contact area only (e.g., Barbosa and Magalhães, 2015; Diserens, 2009; Diserens et al., 2011; O'Sullivan et al., 1999; Wulfsohn and Upadhyaya, 1992). However, the drive mode of a wheel has been shown to affect the shape-characteristics of the tyre-soil contact area. De Pue et al. (2020b) observed a larger contact area in front of the axle than behind the axle of a pulling tyre in a simulation with a discrete element model. Ten Damme et al. (2021b) observed the opposite from field measurements, namely a larger contact area behind the axle than in front of the axle of pulling tractor tyres. In the same field experiment, the authors showed that for pulled tyres, the tyre-soil contact area in front of the axle was longer than or not significantly different from the contact behind the axle (Ten Damme et al., 2021b).

Few authors have investigated the impact of traction on soil deformation. An increase in drawbar pull, with an increase in wheel slip, creates a deeper rut depth (Battiato and Diserens, 2013), and effects of traction on soil deformation have also been observed deeper in the soil profile below the wheel track. Ten Damme et al. (2021a) observed a significantly larger volume of blocked air-filled porosity (0.76 $m^3$ $m^{-3}$ compared to 0.20 $m^3$ $m^{-3}$) and lower Darcian air permeability (1.4 compared to 8.2 $\mu m^2$) at 0.15 m depth for an 11 Mg-tractor pulling at 9.1 kN than at 6.5 kN net drawbar pull. The effect of a higher net drawbar pull on bulk density was, however, negligible (1.55 Mg $m^{-3}$ compared to 1.51 Mg $m^{-3}$) (Ten Damme et al., 2021a). However, the effect of traction on soil deformation cannot be fully understood without knowledge on the effect of traction on the stress distributions beneath the wheel.

Not fully understanding the effect of tractive forces may also explain unexpected differences in the soil response to field traffic. For example, in a Danish soil compaction trial, more subsoil deformation was predicted for a low traction treatment (118 kN wheel load) than for a high traction treatment (73 kN wheel load). However, impact-assessments showed, among others, significantly higher soil penetration resistance in the upper subsoil and significantly reduced cereal grain yield for the 73 kN wheel load-treatment (Schjønning et al., 2016).

Realising the knowledge gaps discussed above, we conducted a field experiment to investigate the effects of traction on the vertical and longitudinal horizontal stress distributions near the tyre-soil interface. The objectives of this study were: i) to compare the tyre-soil contact area and vertical stress distributions for a passive (i.e., rolling) and an active (i.e., pulling) tractor rear tyre, ii) to characterise the horizontal stress distributions for the passive and active tyre, and iii) to explore how the ratio of horizontal to vertical stress varies for the passive and active tyre. The hypotheses were that: a) traction enlarges the tyre-soil contact area, and b) traction decreases vertical stress and increases horizontal stress.

## 2. Materials and methods

### 2.1. Experimental site

Soil stress measurements during wheeling were made in an arable field with cereal stubble at AU Viborg – Research Centre Foulum, Denmark (56°29"N, 9°34"E) in June 2020. The topsoil classifies as a sandy loam; textural data of a neighbouring site are provided in Table 1. The soil water content at 0.10 m depth was 0.26 $m^3$ $m^{-3}$ and thereby slightly more negative than −100 hPa, at which the volumetric soil water content was of 0.28 ± 0.01 $m^3$ $m^{-3}$. The soil water content and the dry bulk density were measured on 36 (nine per block) undisturbed soil cores (100 $cm^3$: 34.82 mm high, 60 mm inner diameter) sampled at 0.10 m depth in reference plots, i.e., parts of the experimental area without traffic. Data for soil cohesion and angle of internal friction (Table 1) were obtained from rotational shear tests, using the shear annulus device as described by Schjønning (1986). Twenty-four samples (six per block) were divided into six groups for shear tests at six different, constant normal loads (σ, kPa): 30, 60, 90, 120, 150 and 180 kPa.

**Table 1**
Soil texture and selected soil physics and mechanical properties of the initial soil conditions.

| Soil depth, m | Texture, g $kg^{-1}$[1] | |
|---|---|---|
| 0–0.25 | Clay | 95 |
| | Silt | 130 |
| | Fine sand | 458 |
| | Coarse sand | 317 |
| | Organic carbon | 18 |
| 0.08–0.11 | Dry bulk density, Mg $m^{-3}$ | 1.36 ± 0.07 |
| | Volumetric soil water content, $m^3$ $m^{-3}$ | 0.26 ± 0.02 |
| | Cohesion, $c$, kPa[2] | 11.3 |
| | Angle of internal friction, tan($\phi$), °[2] | 28.6 |
| | Soil compressive strength, $\sigma_{pc}$, kPa[3] | 99 |

[1] Hansen et al. (2010); [2] obtained from soil cores from the experimental site using the Mohr-Coulomb failure criterion $\tau = \sigma\tan(\phi) + c$, where $\tau$ is the shear stress (kPa) at maximum curvature of the stress-strain curve; [3] estimated using Eq. 6 in Schjønning et al. (2023).

### 2.2. Experimental configurations and set-up

In this study, vertical and horizontal stress measurements were made at 0.10 m depth beneath the right wheels of a tractor without and with traction, i.e., the Passive and Active configuration, respectively (Fig. 1). The tractor had a total load of 85.2 kN (implement included) with a static load of 65.9 kN on the rear axle. The tractor was equipped with low-inflation pressure tyres inflated to 80 kPa (recommended pressure for the load applied to the rear): 520/60 R28 on the front and 650/60 R38 on the rear. For the Passive configuration, the tractor was pulled in neutral gear by a facilitating tractor at a theoretic velocity ($v_t$) of 0.83 m s$^{-1}$. For the Active configuration, the tractor was pulling the facilitating tractor that had a load of 98.8 kN. We ensured high traction on the rear wheels of the Active tractor by disabling the 4WD. The theoretical velocity of the Active tractor was set to 0.83 m s$^{-1}$ and that of the facilitating tractor to 0.56 m s$^{-1}$. Moreover, the facilitating (pulled) tractor had activated the 4WD and was set in gear to induce a braking of the pulling tractor to further ensure a high drawbar pull (*DP*, kN) (Table 2).

Drawbar pull was measured using a strain-gauge transducer connected in between the two tractors. It was measured over a distance of approximately six meters during each pass. The transducer was of the type *Load Link* and consisted of four individual strain-gauges that were placed in a Wheatstone bridge. Measurements were made at a frequency of 0.2 kHz and data were sent to a data logger (HBM eDaq lite). We calculated the arithmetic mean of drawbar pull to indicate the rolling resistance of the Passive configuration and the level of traction, i.e., net drawbar pull, for the Active configuration (Table 2).

A laser-sensor (Fig. 1, Lamandé and Schjønning 2011) kept track of the passing tractor and yielded, in combination with the wheelbase, velocity ($v$, m s$^{-1}$) (Table 2). Velocity was, amongst other things, used to convert duration of the stress measurements to distance. For the Active tractor, wheel slip ($S$, %), was calculated following Koolen and Kuipers (1983) and the traction coefficient ($\mu_{tr}$, -), also known as the drawbar pull to weight ratio, following Battiato and Diserens (2017) (Table 2).

The stress measurements were made in four replicate blocks (Fig. 2). In each block, the two configurations (i.e., active and passive tyre) and a third plot, free from traffic and used for soil sampling for soil physical and mechanical characterisation (Table 1), were randomly distributed. After each pass, the rut width was measured with a ruler in three places in the wheel track for which the stress-recordings were collected.

### 2.3. Stress measurements

Vertical ($\sigma_z$, kPa) and longitudinal (in the driving direction) horizontal ($\sigma_x$, kPa) stresses were derived from stress measurements during wheeling by a front and rear tyre of the Passive and Active tractor (Fig. 1). We used pressure transducers positioned 0.10 m below the pre-traffic soil surface. Each sensor (Fig. 3A) comprised a load cell (DS Europe and X-SENSORS, Series BC-302) embedded in a cylindrical steel transducer housing (ø 52 mm, length 80 mm). A piston (ø 20 mm) transmitted the load to the load cell. The load was converted to pressure (kPa) by dividing the force by the area of the piston. We installed three rows with 10 sensors per plot (Fig. 3). The distance between two load cells, i.e., the spatial resolution across the tyre, was approximately 83 mm. The stress measurements thus covered a width of about 0.75 m, which was wider than the tractors' rear tyres (650/60 R38).

One row of sensors measured the vertical stress and two rows the horizontal stress. For the sensors measuring horizontal stress, all sensors in one row were installed with the load cells facing against the direction of travel (denoted $\sigma_{x1}$) or facing the direction of travel (denoted $\sigma_{x2}$)

**Table 2**
Characteristics of tractor performance for the Passive and Active configurations.

| | Passive tractor | Active tractor |
|---|---|---|
| Theoretical velocity, $v_t$, m s$^{-1}$ | 0.83 | 0.83[1] |
| Velocity, $v$, m s$^{-1}$ | 0.85 ± 0.009 | 0.62 ± 0.006 |
| Rolling resistance, kN | 5.72 ± 0.29 | na[2] |
| Net drawbar pull, *DP*, kN | na | 41.58 ± 1.18 |
| Wheel slip, $S$,%[3] | -3 ± 1.1 | 25 ± 0.7 |
| Traction coefficient, $\mu_{tr}$, -[4] | na | 0.49 ± 0.019 |

[1] The facilitating (pulled) tractor was set to 0.56 m s$^{-1}$ to increase the drawbar pull. [2] not directly measured. [3] $S = 1 - \frac{V}{V_t}$ (Koolen and Kuipers, 1983). [4] $\mu_{tr} = \frac{DP}{W}$, where *DP* is the net drawbar pull and *W* the tractor's weight (Battiato and Diserens, 2017). na = not applicable.

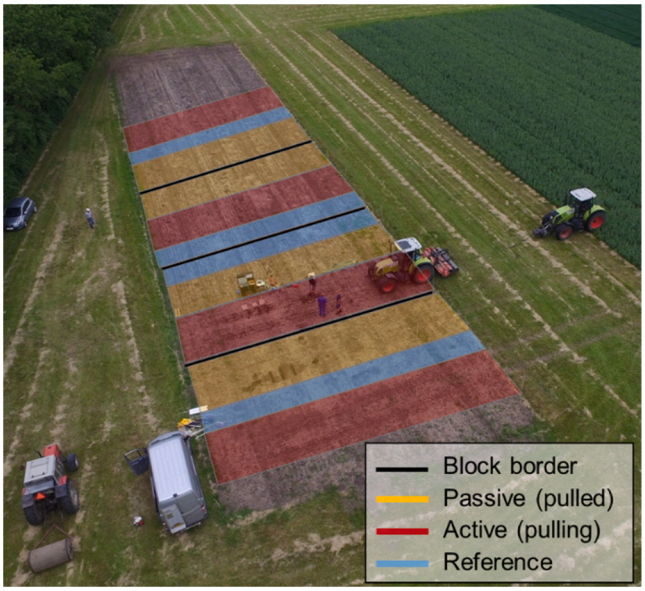


**Fig. 2.** Experimental layout. Photo by Jens Bonderup Kjeldsen.

**Fig. 1.** Set-up in photo and video (QR-codes) of the main and facilitating tractors in the Passive (left) and Active (right) configuration. The white arrows indicate the driving direction. The white oval (left) highlights the laser-sensor (Section 2.2). Photos by Loraine ten Damme.

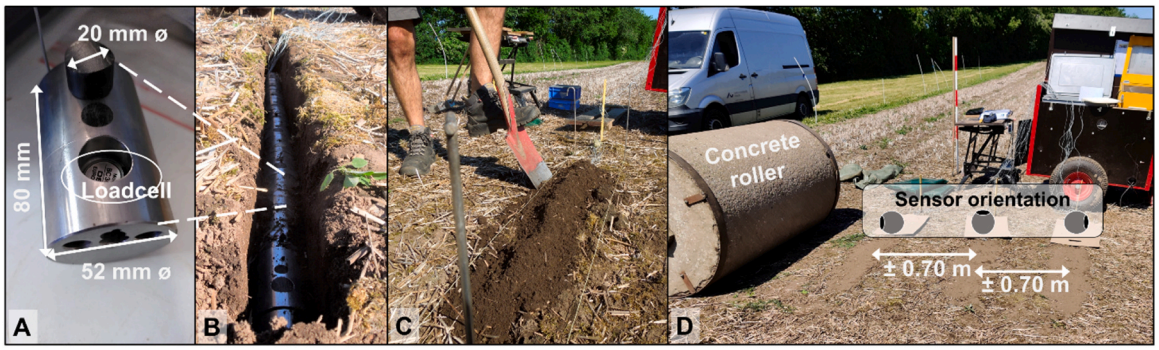


**Fig. 3.** Overview of installation of the stress sensors. See Sections 2.3 and 2.4 for explanation. Photos A–C by Loraine ten Damme, photo D by Jens Bonderup Kjeldsen.

(Fig. 3D). The horizontal use of sensors meant that stress was measured both directly, i.e., when the piston was pushed into the steel housing, and indirectly, i.e., when the steel housing was pushed. For an infinitesimally small sensor, direct and indirect measured stresses would equal each other. Beneath a tyre, the sensors measured the net horizontal stress. If no displacement of transducers occurred, the direction of the net horizontal stress remained unknown.

#### 2.3.1. Installation of the sensors

First, the soil surface was gently scraped clean of loose debris to level the surface. A stencil and a semi-circled Dutch hoe were then used to dig a fitted trench (ø 50 mm) in which the load transducers were placed (Fig. 3B). The trench was dug to 0.12 m depth for horizontal stress measurements and to 0.15 m depth for the vertical stress measurements. The diameter of the Dutch hoe was 2 mm less than the sensors' diameter to ensure a stable fit of the transducers in the trenches.

Due to the cylindrical form of the transducer housings, the lower halves of the pistons of the horizontally orientated sensors were in contact with the soil in the trenches, but the upper halves were not. To increase soil-sensor contact and to minimise differences in soil stiffness in front of the pistons, some soil was firmly pressed in the open corner between the load cell and trench wall. All sensors were covered with the remaining dug-out soil (Fig. 3C). For the vertically orientated sensors, a cut was made from the soil surface towards the sensors (Fig. 3C) to avoid the tyre bridging the undisturbed soil surrounding the sensors, which could lead to an underestimation of the vertical stress. For a uniform finish of the installations and optimised sensor-soil contact, the rows of sensors were rolled over twice by a 1.2 Mg hollow concrete roller (Fig. 3D).

The load cells were connected to a data-acquisition system and measurements were made at 1 kHz. Please consult Lamandé et al. (2007) for details of the measuring system. After completing the measurements in a plot, the soil covering the sensors was removed to define the position of each load cell relative to the centre and the edge of the wheel track.

### 2.4. Assessment of tyre-soil interaction characteristics and distributions of vertical and horizontal stress

#### 2.4.1. Data handling

Some stress recordings showed stress readings long after the tyre had passed. These were discarded. When stress readings from a load cell beneath the wheel rut were missing, due to lack of contact between the soil and the piston, symmetry across the tyre was assumed and missing data replaced. For example, missing readings at 0.1 m on one side of the centreline of the wheel track were replaced with readings from the sensor nearest to 0.1 m on the other side of the centreline of the wheel track. We used 10 kPa to indicate soil-sensor contact and set readings less than 10 kPa to zero. We excluded the data from the second horizontal station ($\sigma_{x2}$) for two Active passes for which we observed a large displacement (>0.05 m) of the stress sensors after traffic. We considered the measurements at both stations (at $\sigma_{x1}$ and $\sigma_{x2}$) as measurements of (net) horizontal stress ($\sigma_x$).

#### 2.4.2. Calculations

The vertical stress measurements were used for estimating the contact area ($A$, $m^2$), the length of the contact area in front of and behind the axle ($l_1$ and $l_2$, respectively, m), the apparent wheel load ($F_{app}$, kN) and the mean ground pressure ($MGP = F_{app}/A$, kPa). Moreover, we derived the maximum vertical stress ($p_{max}$, kPa) and median vertical stress ($p_{median}$, kPa) at 0.1 m depth. The contact area was numerically calculated following Schjønning et al. (2008) with a distance of 83 mm (the distance between two load cells). The apparent wheel load was calculated by integrating the vertical stresses in the contact area. While the apparent wheel load was calculated for the front and rear tyre, the other characteristics were obtained for the rear tyres only. The horizontal stress measurements were used for calculating the area over which horizontal stress was measured ($A_{-x}$, $m^2$) similar to the approach for calculating the contact area based on the vertical stress measurements. The maximum horizontal stress at 0.1 m depth is denoted $p_{max\text{-}x}$ and the median horizontal stress at 0.1 m depth is denoted $p_{median\text{-}x}$.

We calculated the average vertical and average horizontal stress distributions at 0.1 m depth for the Passive and the Active rear tyres. We did so by calculating the arithmetic mean stress (kPa) for each position beneath the tyres across all passes. For detailed discussion of the stress distributions beneath the two configurations, we projected a rectangular grid on the contact area and calculated the average point loads for each grid cell. Each rectangle in the grid measured 10 cm in the driving direction and 8.3 cm across the tyre (i.e., reflected one load cell). Note that these average stress distributions are based on eight or six measurements of horizontal stress (for the Passive and Active configuration, respectively) and on four measurements of vertical stress (for both Passive and Active configurations). The point loads were used to calculate coefficients of variation of the vertical and horizontal stresses beneath the Passive and the Active tyre, i.e., for each grid cell.

Finally, we calculated the ratio of horizontal to vertical stress for each cell in the rectangular grid. A ratio of 1 means that the magnitudes of horizontal and vertical stress in the same position beneath the tyre were similar. At a ratio of <1, vertical stress exceeded the horizontal stress, and at a ratio of >1, horizontal stress exceeded the vertical stress.

### 2.5. Statistical analyses

The differences in drawbar pull within each pass – based on rolling averages with a window size of 100 (amounting to 0.5 s) and moving the window by 0.25 s – tested non-significant when fitted to a linear model ($P > 0.05$). We used the non-parametric Kruskal-test for differences in the mean drawbar pull between the four passes of each configuration.

No significant differences were observed (P ≥ 0.180). The effect of traction on the width of the wheel rut was assessed using a linear model. The effect of traction on the measured tyre-soil interaction characteristics ($F_{app}$, $A$ and $A_{-x}$, $l_1$ and $l_2$, MGP, $p_{max}$ and $p_{max\text{-}x}$, $p_{median}$ and $p_{median\text{-}x}$) and on the ratios of horizontal to vertical stress at 0.1 m depth beneath the central part of the tyre (i.e., excluding the tyre periphery) was analysed using the Kruskal-test. All analyses were done at the level of significance of 0.05.

## 3. Results and discussion

### 3.1. Comparison of static and apparent wheel load

The apparent loads of the Passive and Active rear wheels ($F_{app}$, Table 3) were 24 % and 30 % smaller, respectively, than the 32.9 kN static wheel load. For the front axle, the apparent wheel loads were also smaller than the static wheel load (9.7 kN), by 23 % and 81 % for the Passive and Active configuration, respectively (data not shown). Differences between the static load and the apparent load are commonly found (Lamandé et al., 2015; Schjønning and Lamandé, 2010). Such differences are mainly explained by contrasting soil- and sensor stiffness (Kirby, 1999) and by sensor geometry (Lamandé et al., 2015). This context dependency means that pressure readings are often corrected by a sensor-soil-specific factor $LF = F_{static}/F_{app}$.

In the present study, the apparent rear wheel load was consistently smaller than the static rear wheel load. Minima $F_{static}/F_{app}$ were 1.23 and 1.19 for the Passive and the Active rear tyre, respectively (data not shown). This indicates that the sensors measuring vertical stress could not capture completely the wheel load during wheeling. This may be explained by an observation made, among others, by Pytka (2009), who showed that the transmission of the major principal stress from tyre to soil was not in a vertical direction but tilted forwards. It means that the use of a load factor $F_{static}/F_{app}$ based on solely vertical stress measurements to correct the vertical and horizontal stress measurements would be insufficient. Moreover, Pytka (2009) observed that the major principal stress was tilted further forwards for a rolling than for a driving wheel, i.e., transmitted in a less vertical direction. In our study, the difference in apparent rear wheel load between the Passive and Active configurations was not significant (Table 3, P = 0.564). These contrasting observations may be explained by differences in the experimental setup. Pytka (2009) obtained his results for a truck at nearly 100 % slip on a loess soil, at which conditions the rolling resistance may have been much higher than in our study.

**Table 3**
Tyre-soil interaction characteristics of the rear tyre (static wheel load, $F_{static}$, of 33 kN). Different letters indicate a P < 0.05 between the tyres. The data is presented as geometric means with the geometric standard deviation in brackets.

| | Passive | Active |
|---|---|---|
| $F_{app}$, kN | 25.0 (1.15) a | 23.0 (1.15) a |
| $A$, m$^2$ | 0.38 (1.05) b | 0.48 (1.26) a |
| $l_1$, m | 0.29 (1.21) a | 0.31 (1.37) b |
| $l_2$, m | 0.29 (1.31) a | 0.33 (1.18) b |
| $MGP$, kPa | 65 (1.14) a | 47 (1.38) b |
| $p_{max}$, kPa | 191 (1.16) a | 141 (1.21) b |
| $p_{median}$, kPa | 61 (1.27) a | 54 (1.10) a |
| $A_{-x}$, m$^2$ | 0.58 (1.31) a | 0.74 (1.27) a |
| $p_{max\text{-}x}$, kPa | 122 (1.47) a | 160 (1.37) a |
| $p_{median\text{-}x}$, kPa | 30 (1.25) a | 40 (1.52) a |

$F_{app}$ = apparent wheel load; $A$ = tyre-soil contact area; $l_1$ = length of contact area in front of the axle; $l_2$ = length of contact area behind the axle; $MGP$ = mean ground pressure; $p_{max}$ = maximum vertical stress at 0.1 m depth; $p_{median}$ = median vertical stress at 0.1 m depth; $A_{-x}$ = area over which horizontal stress was measured; $p_{max\text{-}x}$ = maximum horizontal stress at 0.1 m depth; $p_{median\text{-}x}$ = median horizontal stress at 0.1 m depth.

### 3.2. Traction effects on the tyre-soil contact area

The measured contact area ($A$) of the rear tyre was 26 % larger in the Active than in the Passive configuration (Table 3, P = 0.043). The enlargement of the contact area due to traction confirms results reported by Ten Damme et al. (2021b), who measured a larger contact area for the rear tyre of a tractor pulling at 9.1 kN compared to a 6.5 kN net drawbar pull. The authors explained the enlargement of the contact area as having resulted not from a change of the length or width of the contact area, but from a change of the shape of the contact area: the corners of the contact area had, as it were, been pulled outwards and become more square. Ten Damme et al. (2021b) hypothesised that the enlargement may have been a result of a higher tyre deflection in response to a higher wheel load. In our study, the increase in drawbar pull did not yield a measurably higher wheel load as also discussed in Section 3.1, but the larger tyre-soil contact area for the Active tyre does show increased tyre deformation in response to traction.

In this study, traction changed both the length and width of the tyre-soil contact area. The contact area in front of and behind the axle ($l_1$ and $l_2$, respectively) were both longer for the Active than for the Passive tyre (Table 3, P = 0.023 and 0.043 for $l_1$ and $l_2$, respectively). For a given configuration, no significant differences were observed for the length of the contact areas in front of and behind the axle (P = 0.473 for the Passive tyre and 0.371 for the Active tyre). Sheludchenko et al. (2022) hypothesised that for a tyre influenced by drawbar pull, the tyre-soil contact patch in front of a wheel's axle would be longer than the contact area behind the wheel's axle. They reasoned this would be caused by the forward movement of the part of the tyre in front of the wheel.

Ten Damme et al. (2021b) reported on field measurements and found that for active tractor tyres, the contact area was larger behind the axle than in front of the axle, in contrast to the contact area beneath passive trailer tyres that tended to be larger in front of the axle. The data derived from our sensors do not reveal a change of the width of the contact area, but we found that the width of the wheel rut was on average 8 % wider for the Active than the Passive configuration: 0.68 (± 0.008) m and 0.63 (± 0.040) m, respectively (P < 0.001). Our stress measurements did not capture this effect because the lateral edge of the tyre, hence the edge of the tyre-soil contact area, generally ended in-between two sensors.

Models such as SoilFlex (Keller et al., 2007) and FRIDA (Schjønning et al., 2008) include a super-ellipse model to describe the periphery or shape of the tyre-soil contact area (Hallonborg, 1996). This model assumes axes-symmetry, and defines the shape (e.g., more rounded or square) by a parameter $n$ (Keller, 2005). Schjønning et al. (2008) concluded that the super-ellipse is better suited to describe the contact area of different passive tyres. Our results (Table 3) indicate that the super-ellipse model may also be suited for pulling tyres. However, comparison with earlier studies indicate that a clear conclusion of the effect of traction on the size and shape of the tyre-soil contact area, and thereby the suitability use of the super-ellipse model, is lacking.

### 3.3. Vertical stress distributions without and with traction

Traction altered the magnitude of vertical stress and the distribution of vertical stress over the tyre-soil contact area. The mean ground pressure ($MGP$) was 28 % lower for the Active than for the Passive tyre (P = 0.057) due to the increase in the contact area and no evident change of the apparent wheel load (Table 3). The maximum vertical stress ($p_{max}$) was 26 % lower for the Active than for the Passive tyre (P = 0.057) and the median vertical stress ($p_{median}$) did not differ between the two configurations (P = 0.343). This indicates that traction does not affect the magnitude of vertical stress equally over the whole tyre-soil contact area, but mostly reduces the magnitude of the highest stress values.

The vertical stress distribution in the driving direction was changed under the influence of traction (Fig. 4). Beneath the Passive tyre, a single peak vertical stress distribution was found for all positions (sensors)

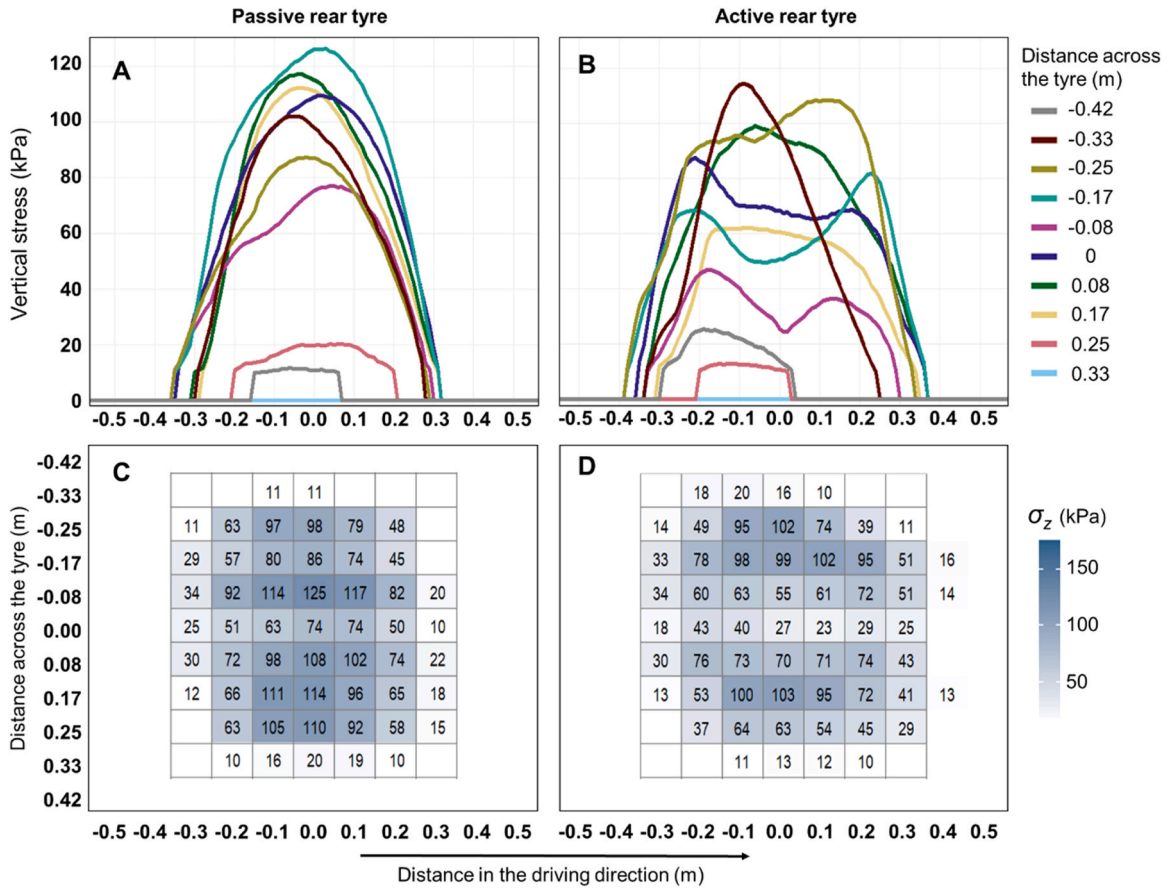


**Fig. 4.** Vertical stress distributions for the rear tyre at 0.1 m depth. AC: Passive tyre. BD: Active tyre. Along the x-axes, the stress distributions in the driving direction is shown, where x = 0 is the axle and x < 0 reflects the stress readings made behind the axle. In A and B, the y-axes show the magnitude of vertical stress and the lines the distance across the tyre, where zero is nearest to the tyre's centreline. In C and D, the y-axes show the distance across the tyre.

across the tyre (Fig. 4A). Beneath the Active tyre, single peak stress distributions occurred near the lateral edges of the tyre, whereas the stress distribution was characterised by plateaus and dual peaks beneath the central part of the Active tyre (Fig. 4B). For the Passive tyre the vertical stress peaked near the axle (i.e., at x ~ 0), while for the Active tyre it peaked at greater distance from the axle, mostly behind the axle (i.e., where x < 0). Across the tyre, a dual peak vertical stress distribution, i.e., with highest values for the area between the tyre's edges and centreline at y = 0.0 m, was observed for both configurations. The dual peak was, however, more pronounced for the Active than for the Passive tyre (Fig. 4CD). A dual peak stress distribution across the tyre signifies tyre deflection (Schjønning et al., 2012), which has been shown to reduce vertical stress in the soil profile (Schjønning et al., 2008).

The coefficient of variation in the central part beneath the tyre (-0.2 $\leq$ x $\geq$ 0.2 and $-0.25 \leq$ y $\geq$ 0.25, with x being the distance in the driving direction and y across the tyre), yielded average coefficients of variation of 45 % and 53 % for the Passive and the Active tyre, respectively. This indicates that the variation in the stress distribution between the individual passes was smaller for the Passive than for the Active configuration. In other words, the tyre with tractive forces had a more variable vertical stress distribution in the tyre-soil contact area than the tyre rolling passively over the soil. This observation aligns with Ten Damme et al. (2021b), who suggested that the more dynamic vertical stress distribution beneath a tyre with (more) traction reflects the way the tyre works when it has to pull.

The changes in the vertical stress distribution in the contact area imply a large effect of drawbar pull on tyre-soil interaction. Such effects are not accounted for in risk assessment methods like SoilFlex (Keller et al., 2007), SOCOMO (Van den Akker, 2004) and Terranimo (Stettler et al., 2014). An important reason is that few of studies on the vertical contact stress distribution have focussed on tyres during traction or braking (e.g., Keller and Arvidsson, 2004; Lamandé and Schjønning, 2008; Raper et al., 1995; Schjønning et al., 2015, 2012). The vertical stress distribution of a tyre without additional forces can be well predicted from tyre- and loading characteristics, but we currently lack models that predict contact stresses for tyres influenced by traction.

### 3.4. Horizontal stress distributions without and with traction

Traction changed the magnitude of horizontal stress and the area over which horizontal stresses were measured (Table 3, Fig. 5). The horizontal stress peaked at a higher level beneath the Active than the Passive tyre (Fig. 5). Both the maximum horizontal stress ($p_{max\text{-}x}$) and the median horizontal stress ($p_{median\text{-}x}$) were considerably higher for the Active than for the Passive tyre (by 40 % and 33 %) (Table 3), yet Ps in the statistical tests exceeded 0.1 due to large variations between individual passes, particularly beneath the Passive tyre. Similarly, the area over which horizontal stress was measured ($A_{.x}$) was 20 % larger for the Active than for the Passive tyre (Table 3), but Ps also exceeded 0.1.

The shapes of the distributions of horizontal stress at 0.1 m depth beneath the Passive and Active tyre were relatively comparable (Fig. 5). Both showed a single peak in the driving direction with the maximum stresses measured behind the axle (i.e., x < 0). Across the tyre, no obvious pattern in the distribution of horizontal stress was observed (Fig. 5CD). The mean coefficient of variation of the horizontal stress in the central part beneath the tyre (-0.2 $\leq$ x $\geq$ 0.2 and $-0.25 \leq$ y $\geq$ 0.25) was 60 % for the Passive and 43 % for the Active tyre. Thus, the horizontal stress distribution varied more between the different passes for

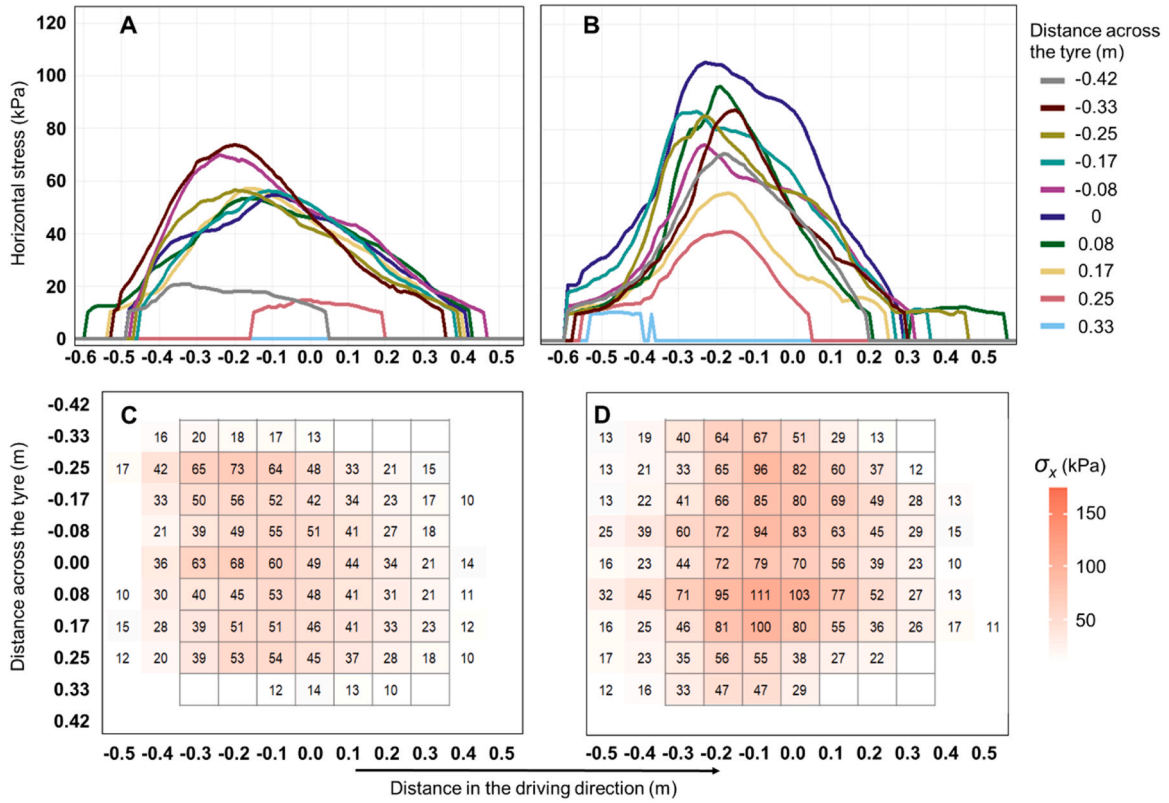


**Fig. 5.** Average horizontal stress distribution for the rear tyre at 0.1 m depth. AC: Passive tyre. BD: Active tyre. Along the x-axes, the stress distributions in the driving direction is shown, where x = 0 is the axle and x < 0 reflects the stress readings made behind the axle. In A and B, the y-axes show the magnitude of horizontal stress and the lines the distance across the tyre, where zero is nearest to the tyre's centreline. In C and D, the y-axes show the distance across the tyre.

the Passive than for the Active configuration, contrary to the vertical stress distribution (Section 3.3).

While both vertical and horizontal stresses tended to peak behind the axle, stresses did not peak spatially aligned. Moreover, our results show that horizontal stresses influenced a larger area of soil than vertical stress, predominantly at greater distance to the rear of the axle. This was found for both the Passive and Active tyres, although more evident for the latter. Beneath the Active tyre, at $x < -0.3$, i.e., at 30 cm and further behind the axle, the average horizontal stresses ranged from 12–45 kPa, whereas no vertical stress was recorded. These findings challenge the assumption that the horizontal stress distribution at the tyre-soil interface is uniform or linear (from front to rear) such as implemented in SOCOMO (Van den Akker, 2004) and SoilFlex (Keller et al., 2007).

### 3.5. The ratio of horizontal to vertical stress

Fig. 6 shows the distribution of the ratio of horizontal stress over vertical stress beneath the tyres, based on the average stress distributions (Figs. 4 and 5) for observations where both stresses were recorded. The ratio horizontal over vertical stress was higher beneath the Active than beneath the Passive tyre, resulting from the decrease in vertical stress and increase in horizontal stress when subjected to traction (Sections 3.3 and 3.4).

Excluding the tyre periphery (outlined by the dashed line in Fig. 6) where stresses were relatively low and hence the ratios uncertain, the ratio of horizontal to vertical stress was significantly higher beneath the Active than beneath the Passive tyre ($P < 0.001$). The ratio ranged from 0.3–1.3 with a median of 0.5 for the Passive tyre and from 0.5–2.6 with a median of 1.0 for the Active tyre. In other words, vertical stress generally exceeded horizontal stress locally (ratio <1) beneath the Passive tyre, while the horizontal stress exceeded the vertical stress (ratio >1) beneath a large part of the Active tyre. A ratio of >1 was found beneath the Active tyre's centreline (i.e., at y = 0) where the magnitude of vertical stress was relatively low (Fig. 4). Moreover, a ratio of >1 dominated to the rear of the axle (i.e., at $x < 0.0$) for the Active tyre but not for the Passive tyre (Fig. 6). This result supports the theory of Yong and Foda (1990), who argued that differences in tyre-soil interaction between a rolling and pulling tyre will manifest on the rear part in the tyre-soil contact area, as this would be the part that contributes to forward movement.

Fig. 6A shows that the ratio of horizontal to vertical stress under the central part of the tyre is relatively stable under the Passive tyre. Following these results, the horizontal stress distribution beneath the central part of a rolling tyre may be estimated following the same distribution as the vertical stress, such as is optional in SOCOMO (Van den Akker, 2004; van den Akker and Van Wijk, 1987) and SoilFlex (Keller et al., 2007).

The differences in the ratio of horizontal to vertical stress between the two configuration and the difference in the distribution of the ratio beneath the tyres highlight the importance of focussing on different drive modes in assessments of the stress-state beneath a tyre. Comparison with earlier research indicates that the size of tyre and/or machine may influence the ratio of horizontal to vertical too. For example, Calleja-Huerta et al. (2023) obtained a ratio of maximum horizontal to vertical stress of approximately 0.3 at 0.10 m depth during wheeling by a field robot equipped with 320/65R16-tyres inflated to 60–90 kPa. In a modelling exercise, Acquah and Chen (2023) also found a ratio of approximately 0.3 at 0.10–0.15 m depth for a small, highly inflated tyre assuming minor wheel slippage.

## 4. Perspectives for soil compaction risk assessments

Currently, online soil compaction risk assessments tools such as Terranimo ® (Schjønning and Lamandé, 2020; Stettler et al., 2014)

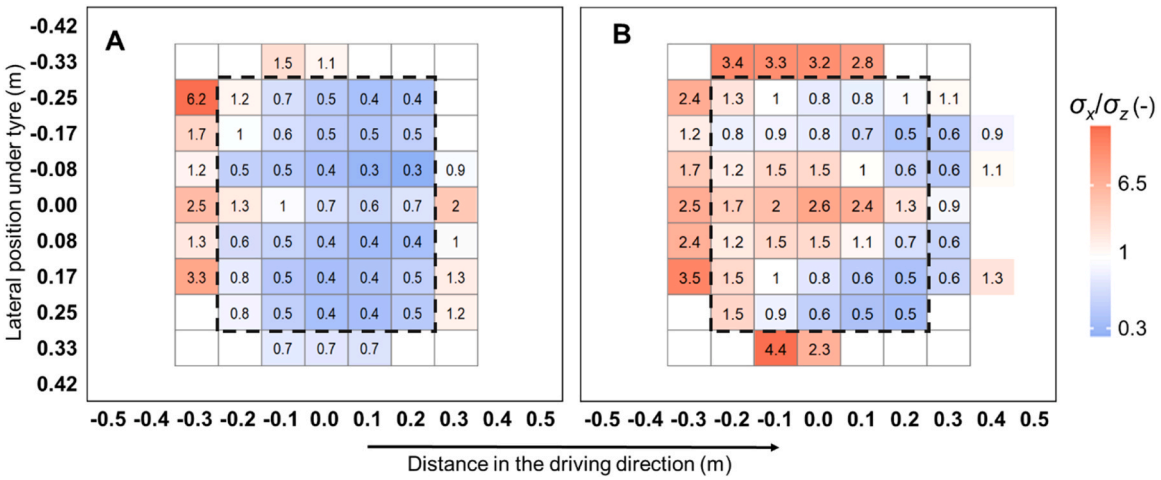


**Fig. 6.** Distribution of the ratio of horizontal to vertical stress beneath the Passive (A) and Active tyre (B). Based on Figs. 4CD and 5CD. The dashed line marks the tyre periphery.

imply comparison between the vertical stress and soil compressive strength. In such models, the former is estimated from the contact area and the vertical stress distribution in a static loading condition. Our data indicate that this approach is insufficient for pulling tyres (Sections 3.1–3.5). We have identified the following research needs to advance the understanding and prediction of the risk of soil deformation for pulling tyres:

1. Further investigations of the shape of the tyre-soil contact area for tyres with different loading characteristics and drawbar pull on various soil conditions are needed. This is because existing research does not provide a conclusive answer on whether the enlargement of the tyre-soil contact area under the influence of traction occurs through a change of the length, width and/or shape of the contact area.
2. More studies should be carried out to investigate further the effects of traction on the distribution of vertical stress in the contact area as accounting for changes of traction on the contact area alone will not yield an accurate distribution of vertical stress beneath wheels with traction. Such investigations may then be used to adapt models now used for passive tyres so they work for pulling tyres too.
3. The effect of the level of traction on the distribution of the ratio of horizontal to vertical stress beneath the tyre should be investigated for different loading and soil conditions. The ratio of horizontal to vertical stress may be used to estimate the horizontal stress from vertical stress distribution, but a single value should be used with caution.
4. The potential benefit of integrating other factors than the vertical stress and strength components in risk assessments for pulling tyres should be explored. Given the effect of traction on the stress-state beneath the tyre, the inclusion of, for example, horizontal stress to a horizontally measured compressive strength may enhance the accuracy of assessments.

## 5. Conclusion

This study showed that traction modifies the tyre-soil interaction significantly and the hypotheses were supported. Under traction, the tyre-soil contact area enlarged, and with no change in wheel load, the mean ground pressure was reduced. The distribution of vertical stress in the contact area changed under the influence of traction and could not be described by the axes-symmetrical approach typically used for passive tyres. Horizontal stress increased significantly under the influence of traction, but the distribution of horizontal stress beneath the passive and active tyre were both characterised by peaking at some distance behind the axle. Under the central part of the tyre, the ratio of horizontal to vertical stress was significantly higher for the tyre with traction, and these observations are important regarding the prediction of soil deformation under a rolling tyre. We suggest further investigations of the tyre-soil interaction including i) the shape of the tyre-soil contact area for tyres with different loading characteristics and drawbar pull on various soil conditions, ii) the effects of traction on the distribution of vertical stress in the contact area to adapt models now used for passive tyres to pulling tyres, and iii) the effect of the level of traction on the distribution of the ratio of horizontal to vertical stress beneath the tyre.

## Funding

This work was funded by the Ministry of Environment and Food of Denmark via the COMMIT project (GUDP Grant no. 34009-16-1086) via the SOLGRAS project (GUDP Grant no. 34009-21-1850).

## CRediT authorship contribution statement

**Loraine ten Damme**: Writing – review & editing, Writing – original draft, Visualization, Project administration, Methodology, Investigation, Formal analyses, Data curation, Conceptualization. **Alvaro Calleja-Huarta**: Writing – review & editing. **Lars Juhl Munkholm**: Writing – review & editing, Supervision, Methodology, Funding acquisition, Conceptualization, Project administration. **Per Schjønning**: Writing – review & editing, Methodology. **Thomas Keller**: Writing – review & editing, Methodology, Conceptualization. **Mathieu Lamandé**: Writing – review & editing, Supervision, Methodology, Investigation, Funding acquisition, Conceptualization, Project administration.

## Declaration of Competing Interest

We declare that we have no known competing financial interests or personal relationships that could have appeared to influence the work reported in this manuscript.

## Data availability

Data will be made available on request.

## Acknowledgements

We owe many thanks to the technical staff at Foulumgaard for their contributions to the field experiment, in particular to Jens Bonderup Kjeldsen, René Mosgaard Madsen, Arne Grud and Søren Anton Kirk

Nielsen for offering the site, organising the machinery and driving the tractors. Jens Kr. Kristensen, who organised the measurements of drawbar-pull, and Gitana Mockuté who assisted with the cables and soil samples, are warmly thanked. Last but not least, we are as grateful as always for the help of Stig T. Rasmussen, who helped pre-, peri and post the field experiment.

## References

Acquah, K., Chen, Y., 2023. Discrete element modelling of soil pressure under varying number of tire passes. J. Terra 107, 23–33. https://doi.org/10.1016/j.jterra.2023.02.003.

Arvidsson, J., Sjöberg, E., van den Akker, J.J.H., 2003. Subsoil compaction by heavy sugarbeet harvesters in southern Sweden III. Risk assessment using a soil water model. Soil Tillage Res. 73, 77–87. https://doi.org/10.1016/S0167-1987(03)00101-6.

Bailey, A.C., Raper, R.L., Way, T.R., Burt, E.C., Johnson, C.E., 1996. Soil stress state under a tractor tire at various loads and inflation pressures. J. Terra 33. https://doi.org/10.1016/S0022-4898(96).

Barbosa, L.A.P., Magalhães, P.S.G., 2015. Tire tread pattern design trigger on the stress distribution over rigid surfaces and soil compaction. J. Terra 58, 27–38. https://doi.org/10.1016/j.jterra.2014.12.006.

Battiato, A., Diserens, E., 2013. Influence of tyre inflation pressure and wheel load on the traction performance of a 65 kW MFWD tractor on a cohesive soil. J. Agric. Sci. 5 https://doi.org/10.5539/jas.v5n8p197.

Battiato, A., Diserens, E., 2017. Tractor traction performance simulation on differently textured soils and validation: a basic study to make traction and energy requirements accessible to the practice. Soil Tillage Res. 166, 18–32. https://doi.org/10.1016/j.still.2016.09.005.

Boussinesq, J., 1885. Application des potentiels à l'étude de l'équilibre et des mouvement des solides élastiques. Gauthier-Villars, Paris, France.

Calleja-Huerta, A., Lamandé, M., Green, O., Munkholm, L.J., 2023. Vertical and horizontal stresses from a lightweight autonomous field robot during repeated wheeling. Soil Tillage Res. 233 https://doi.org/10.1016/j.still.2023.105790.

ten Damme, L., Schjønning, P., Munkholm, L.J., Green, O., Nielsen, S.K., Lamandé, M., 2021b. Traction and repeated wheeling – effects on contact area characteristics and stresses in the upper subsoil. Soil Tillage Res. 211 https://doi.org/10.1016/j.still.2021.105020.

ten Damme, L., Schjønning, P., Munkholm, L.J., Green, O., K. Nielsen, S., Lamandé, M., 2021a. Soil structure response to field traffic: effects of traction and repeated wheeling. Soil Tillage Res. 213, 105128 https://doi.org/10.1016/j.still.2021.105128.

De Pue, J., Lamandé, M., Schjønning, P., Cornelis, W.M., 2020b. DEM simulation of stress transmission under agricultural traffic Part 3: Evaluation with field experiment. Soil Tillage Res. 200, 104606 https://doi.org/10.1016/j.still.2020.104606.

De Pue, J., Lamandé, M., Cornelis, W., 2020a. DEM simulation of stress transmission under agricultural traffic Part 2: shear stress at the tyre-soil interface. Soil Tillage Res. 203 https://doi.org/10.1016/j.still.2020.104660.

van den Akker, J.J.H., 2004. SOCOMO: A soil compaction model to calculate soil stresses and the subsoil carrying capacity. Soil Tillage Res. 79, 113–127. https://doi.org/10.1016/j.still.2004.03.021.

van den Akker, J.J.H., van Wijk, A.L.M., 1987. A model to predict subsoil compaction due to field traffic, in: Monnier, G., Goss, M.J. (Eds.), Soil Compaction and Regeneration. Proceedings of the Workshop on Soil Compaction: Consequences and Structural Regeneration Processes/Avignon 17–18 September, 1985. A.A. Balkema, Rotterdam, Boston, Pp. 69–84.

Diserens, E., 2009. Calculating the contact area of trailer tyres in the field. Soil Tillage Res. 103, 302–309. https://doi.org/10.1016/j.still.2008.10.020.

Diserens, E., Défossez, P., Duboisset, A., Alaoui, A., 2011. Prediction of the contact area of agricultural traction tyres on firm soil. Biosyst. Eng. 110, 73–82. https://doi.org/10.1016/j.biosystemseng.2011.06.008.

Håkansson, I., Reeder, R.C., 1994. Subsoil compaction by vehicles with high axle load-extent, persistence and crop response. Soil Tillage Res. 29, 277–304. https://doi.org/10.1016/0167-1987(94)90065-5.

Hallonborg, U., 1996. Super ellipse as tyre-ground contact area. J. Terra 33, 125–132. https://doi.org/10.1016/S0022-4898(96)00013-4.

Horn, R., Peth, S., 2011. Mechanics of Unsaturated Soils for Agricultural Applications. Kiel 1–30. https://doi.org/10.1007/978-1-84996-417-3.

Horn, R., Blackwell, P.S., White, R., 1989. The effect of speed of wheeling on soil stresses, rut depth and soil physical properties in an ameliorated transitional red-brown earth. Soil Tillage Res. 13, 353–364. https://doi.org/10.1016/0167-1987(89)90043-3.

Horn, R., Richards, B.G., Gräsle, W., Baumgartl, T., Wiermann, C., 1998. Theoretical principles for modelling soil strength and wheeling effects - a review. Z. fur Pflanzenernahr. und Bodenkd. 161, 333–346.

Keller, T., 2005. A Model for the prediction of the contact area and the distribution of vertical stress below agricultural tyres from readily available tyre parameters. Biosyst. Eng. 92, 85–96. https://doi.org/10.1016/j.biosystemseng.2005.05.012.

Keller, T., Arvidsson, J., 2004. Technical solutions to reduce the risk of subsoil compaction: effects of dual wheels, tandem wheels and tyre inflation pressure on stress propagation in soil. Soil Tillage Res. 79, 191–205. https://doi.org/10.1016/j.still.2004.07.008.

Keller, T., Défossez, P., Weisskopf, P., Arvidsson, J., Richard, G., 2007. SoilFlex: A model for prediction of soil stresses and soil compaction due to agricultural field traffic including a synthesis of analytical approaches. Soil Tillage Res. 93, 391–411. https://doi.org/10.1016/j.still.2006.05.012.

Keller, T., Sandin, M., Colombi, T., Horn, R., Or, D., 2019. Historical increase in agricultural machinery weights enhanced soil stress levels and adversely affected soil functioning. Soil Tillage Res. 194, 12. https://doi.org/10.1016/j.still.2019.104293.

Kirby, J.M., 1999. Soil stress measurement: Part I. transducer in a uniform stress field. J. Agric. Eng. Res. 72, 151–160.

Koolen, A.J., Kuipers, H., 1983. Agricultural Soil Mechanics. Springer-Verlag Berlin and Heidelberg GmbH & Co (KG).

Lamandé, M., Schjønning, P., 2008. The ability of agricultural tyres to distribute the wheel load at the soil-tyre interface. J. Terra 45, 109–120. https://doi.org/10.1016/j.jterra.2008.09.004.

Lamandé, M., Schjønning, P., 2011. Transmission of vertical stress in a real soil profile. Part II: effect of tyre size, inflation pressure and wheel load. Soil Tillage Res. 114, 71–77. https://doi.org/10.1016/j.still.2010.08.011.

Lamandé, M., Schjønning, P., Tøgersen, F.A., 2007. Mechanical behaviour of an undisturbed soil subjected to loadings: Effects of load and contact area. Soil Tillage Res. 97, 91–106. https://doi.org/10.1016/j.still.2007.09.002.

Lamandé, M., Keller, T., Berisso, F.E., Stettler, M., Schjønning, P., 2015. Accuracy of soil stress measurements as affected by transducer dimensions and shape. Soil Tillage Res. 145, 72–77. https://doi.org/10.1016/j.still.2014.08.011.

O'Sullivan, M.F., Henshall, J.K., Dickson, J.W., 1999. A simplied method for estimating soil compaction. Soil Tillage Res. 49, 325–335.

Peth, S., Horn, R., 2006. The mechanical behavior of structured and homogenized soil under repeated loading. J. Plant Nutr. Soil Sci. 169, 401–410. https://doi.org/10.1002/jpln.200521942.

Pytka, J., 2005. Effects of repeated rolling of agricultural tractors on soil stress and deformation state in sand and loess. Soil Tillage Res. 82, 77–88. https://doi.org/10.1016/j.still.2004.06.005.

Pytka, J., 2009. Determining and analysing the stress state under wheeled-vehicle loads. Proc. Inst. Mech. Eng. Part D. J. Automob. Eng. 223, 233–253. https://doi.org/10.1243/09544070JAUTO880.

Raper, R.L., Bailey, A., Burt, E.C., Way, T.R., Liberati, P., 1995. Inflation pressure and dynamic load effects on soil deformation and soil-tire interface stresses. Trans. ASAE 38, 685–689.

Schjønning, P., 1986. Shear strength determination in undisturbed soil at controlled water potential. Soil Tillage Res. 8, 171–179. https://doi.org/10.1016/0167-1987(86)90332-6.

Schjønning, P., Lamandé, M., 2010. A note on the vertical stresses near the soil-tyre interface. Soil Tillage Res. 108, 77–82. https://doi.org/10.1016/j.still.2010.03.006.

Schjønning, P., Lamandé, M., 2020. An introduction to Terranimo® (⟨www.terranimo.dk⟩). Unpublished note, Aarhus University, Dept. Agroecology [WWW Document]. URL ⟨https://terranimo.dk/⟩ (accessed 5.8.24).

Schjønning, P., Lamandé, M., Tøgersen, F.A., Arvidsson, J., Keller, T., 2008. Modelling effects of tyre inflation pressure on the stress distribution near the soil-tyre interface. Biosyst. Eng. 99, 119–133. https://doi.org/10.1016/j.biosystemseng.2007.08.005.

Schjønning, P., Lamandé, M., Keller, T., Pedersen, J., Stettler, M., 2012. Rules of thumb for minimizing subsoil compaction. Soil Use Manag. 28, 378–393. https://doi.org/10.1111/j.1475-2743.2012.00411.x.

Schjønning, P., Stettler, M., Keller, T., Lassen, P., Lamandé, M., 2015. Predicted tyre-soil interface area and vertical stress distribution based on loading characteristics. Soil Tillage Res. 152, 52–66. https://doi.org/10.1016/j.still.2015.03.002.

Schjønning, P., Lamandé, M., Munkholm, L.J., Lyngvig, H.S., Nielsen, J.A., 2016. Soil precompression stress, penetration resistance and crop yields in relation to differently-trafficked, temperate-region sandy loam soils. Soil Tillage Res. 163, 298–308. https://doi.org/10.1016/j.still.2016.07.003.

Seehusen, T., Riley, H., Riggert, R., Fleige, H., Børresen, T., Horn, R., Zink, A., 2014. Traffic-induced soil compaction during manure spreading in spring in South-East Norway. Acta Agric. Scand. Sect. B — Soil Plant Sci. 64, 220–234. https://doi.org/10.1080/09064710.2014.902097.

Sheludchenko, B., Šarauskis, E., Kukharets, S., Zabrodskyi, A., 2022. Graphic analytical optimization of design and operating parameters of tires for drive wheels of agricultural machinery. Soil Tillage Res. 215 https://doi.org/10.1016/j.still.2021.105227.

Soane, B.D., Blackwell, P.S., Dickson, J.W., Painter, D.J., 1981. Compaction by agricultural vehicles: a review II. Compaction under tyres and other running gear. Soil Tillage Res 1, 373–400. https://doi.org/10.1016/0167-1987(80)90039-2.

Söhne, W., 1953. Druckverteilung im Boden und Bodenverformung unter Schlepperreifen. (Pressure distribution in the soil and soil deformation under tractor tyres). Grundl. der Landtech. 49, 63.

Stettler, M., Keller, T., Weisskopf, P., Lamandé, M., Lassen, P., Schjønning, P., 2014. Terranimo ® - a web-based tool for evaluating soil compaction. Landtechnik 69, 132–137.

Way, T.R., Erbach, D.C., Bailey, A.C., Burt, E.C., Johnson, C.E., 2005. Soil displacement beneath an agricultural tractor drive tire. J. Terra 42, 35–46. https://doi.org/10.1016/j.jterra.2004.06.001.

Wiermann, C., Way, T.R., Horn, R., Bailey, A.C., Burt, E.C., 1999. Effect of various dynamic loads on stress and strain behavior of a Norfolk sandy loam. Soil Tillage Res. 50, 127–135. https://doi.org/10.1016/S0167-1987(98)00199-8.

Wulfsohn, D., Upadhyaya, S.K., 1992. Determination of dynamic three-dimensional soil-tyre contact profile. J. Terra 29, 433–464. https://doi.org/10.1016/0022-4898(92)90046-M.

Yong, R.N., Foda, M.A., 1990. Tribology model for determination of shear stress distribution along the tyre-soil interface. J. Terra 27, 93–114.